Aberystwyth University

Natural and laboratory TT-OSL dose response curves: testing the lifetime of the TT-OSL signal in nature
Chapot, M. S.; Roberts, H. M.; Duller, G. A. T.; Lai, Z. P.

Accepted Manuscript

Natural and laboratory TT-OSL dose response curves: testing the lifetime of the TT-OSL signal in nature

M.S. Chapot, H.M. Roberts, G.A.T. Duller, Z.P. Lai

Natural and laboratory TT-OSL dose response curves: testing the lifetime of the TT-OSL signal in nature

M.S. Chapot,[1*] H.M. Roberts,[1] G.A.T. Duller,[1] and Z.P. Lai[2]

[1]*Department of Geography and Earth Sciences, Aberystwyth University, Aberystwyth, SY23 3DB, U.K.*
[2]*School of Earth Sciences, China University of Geosciences,Wuhan, 430074, China*
corresponding author (msj1@aber.ac.uk)
Tel: 44 (0) 1970 622606

Abstract

This study compares natural and laboratory generated thermally transferred optically stimulated luminescence (TT-OSL) dose response curves (DRCs) for fine-grain quartz extracts from the Luochuan loess section in central China. Both DRCs saturate at high doses relative to the quartz OSL signal; the natural TT-OSL DRC saturates at about 2200 Gy and laboratory DRCs saturate at about 2700 Gy. However, the natural and laboratory TT-OSL DRCs deviate from one another at circa 150 Gy resulting in TT-OSL equivalent dose underestimation relative to palaeodoses expected from dose rates and independent age control. The lifetime of the TT-OSL signal at 10 °C, calculated from values of trap parameters E and s, is compared against the value for lifetime of the TT-OSL signal in nature at average burial temperature as determined from the age underestimation caused by deviation of the natural and laboratory generated DRCs. These two independent assessments of TT-OSL signal lifetime at Luochuan give similar values, suggesting that laboratory measurements of thermal stability reflect natural burial lifetimes and can potentially be used to correct TT-OSL ages for the difference between natural and laboratory dose response curves.

Keywords

Natural DRC, TT-OSL, Thermal stability, Chinese loess, Quartz

1. Introduction

Luminescence dating techniques rely on the assumption that luminescence signal response to irradiation within a laboratory resembles the signal response to irradiation in a natural environment. Recent studies have demonstrated that this assumption is testable through comparing laboratory dose response curves with natural dose response curves (e.g. Chapot et al, 2012). While laboratory dose response curves are constructed by plotting normalised luminescence intensities against administered radiation doses, natural dose response curves require a suite of known age samples for which normalised luminescence intensities can be plotted against expected palaeodose (i.e. the radiation dose that is estimated to have accumulated during burial based on independent age control and dose rate measurements). This study compares natural and laboratory dose response curves of the thermally transferred optically stimulated luminescence (TT-OSL) signal from fine grain quartz extracts of a suite of samples from the Luochuan loess section of the Chinese Loess Plateau.

The quartz TT-OSL signal was introduced as a dosimeter for dating sediments by Wang et al. (2006) and has been suggested to be able to date beyond the age range of the quartz OSL signal (Duller and Wintle, 2012). Attempts to date old samples with the TT-OSL signal have had mixed results, with some studies reporting agreement with independent age control (e.g. Pickering et al., 2013) and others reporting age underestimation (e.g. Thiel et al., 2012). Wang et al. (2006) reported TT-OSL equivalent dose underestimation for four samples bracketing the Brunhes-Matayuma paleaomagnetic boundary (~775 ka), unless a pulsed irradiation procedure was applied, in which case, the pulsed irradiated TT-OSL ages agreed with the independent age control.

Pulsed irradiation procedures involve administering laboratory radiation doses in discrete pulses with a heat treatment in between. For example, 2000 seconds of exposure to a radiation source, may be divided into 10 pulses of 200 seconds exposure with the aliquot heated to 240 °C for 10 seconds between each pulse. The pulsed irradiation technique was proposed by Bailey (2004) for the fast component quartz OSL signal in order for charge competition during laboratory irradiations to be similar to the low intensity, long duration radiation exposure in natural burial environments. However, Chapot et al. (2014) investigated pulsed irradiation procedures for TT-OSL protocols and

they suggest that inter-pulse heat treatments during the pulsed irradiation procedures thermally deplete the TT-OSL signal and should not be used for TT-OSL dating purposes.

Agreement between TT-OSL and fast component quartz OSL ages has been reported in a number of studies (e.g. Arnold et al., in press and references therein). At Luochuan, fast component OSL and TT-OSL ages are reported to be consistent for samples with equivalent doses up to ~400 Gy (Wang et al., 2006). However, the reliability of OSL equivalent doses >150 Gy can be questioned at this site (Chapot et al., 2012) as OSL ages have been observed to underestimate independent age control (e.g. Buylaert et al. 2007, Lai 2010, Chapot et al. 2012). This fast component OSL age underestimation cannot be resolved by component fitting or using a multiple aliquot regenerative protocol (Chapot et al., 2012) and suggests the possibility that TT-OSL and fast component OSL ages can be in agreement but both underestimate the actual burial age. Even still, consistent fast component OSL and TT-OSL ages can also be in agreement with independent age control (e.g. samples at Luochuan with equivalent doses < 150 Gy) and it is uncertain whether any observed underestimation is caused by the same or differing mechanisms (e.g. uncorrected sensitivity change, low thermal stability, etc).

1.1 Previous investigations characterising TT-OSL source traps

Characterisation of the kinetic parameters (E and s) of the source traps for TT-OSL signals and their associated thermal stabilities has been investigated by several research groups (e.g. Li and Li, 2006; Adamiec et al., 2010; Shen et al., 2011). Li and Li (2006) identified three thermal transfer source traps that they refer to as shallow, medium and deep. The TT-OSL signal used for dating corresponds to the medium trap of that study, which is reported to have an E value of 1.14 ± 0.05 eV and an s value on the order of $10^{6.2}$ s^{-1} (Table 1a) based on an isothermal test and Arrhenius plot (Table 2). The signal lifetime at 10 °C corresponding to these trap parameters is 3.7 Ma (Table 1a).

Adamiec et al. (2010) identified two TT-OSL source traps that they refer to as recuperated OSL (Re-OSL) and basic transfer (BT-OSL), following the nomenclature of Wang et al. (2006). The theoretical basis of the Re-OSL and BT-OSL signals presented by Wang et al. (2006) was that the Re-OSL signal originated from a double transfer mechanism involving the fast component OSL trap and

the BT-OSL signal originated by single transfer from optically insensitive traps with a near-endless supply of electrons. Wang et al. (2006) initially separated these two TT-OSL signals by measuring multiple thermal transfers (preheat/ optical stimulation cycles) until the TT-OSL signal reached a low intensity plateau. The plateau defined the BT-OSL signal while the first TT-OSL cycle intensity minus the BT-OSL signal defined the Re-OSL signal. Adamiec et al. (2010) suggested that the Re-OSL signal has a lifetime of 4.5 Ma at 10 °C (E = 1.46 eV, s = 7.6 x 10^{11} s^{-1}; Table 1a), whereas the BT-OSL signal has a lifetime of 4800 Ma at the same temperature (E = 1.72 eV, s = 2.9 x 10^{12} s^{-1}), based on Arrhenius plots constructed following Hoogenstraten's method of measuring TL curves with variable heating rates (Table 2).

Shen et al (2011) identified three TT-OSL source traps that they referred to as A, B, and D (Trap C refers to the fast component OSL trap). Trap A is suggested to be the primary source trap accounting for ~80% of the TT-OSL signal used in dating protocols. Traps B and D are thought to each provide ~10% of the signal. Traps A and B are suggested to be sources for single transferred charge, while Trap D is a refuge trap for a double transfer mechanism involving the fast component OSL trap (Shen et al., 2011). The primary source, Trap A, is reported to have a lifetime of about 0.24 Ma at 10 °C (E = 1.34 ± 0.05 eV, s = 10^{11} s^{-1}; Table 1a), whereas Trap B has a lifetime of about 8500 Ma at the same temperature (E = 1.66 ± 0.07 eV, s = 10^{12} s^{-1}). Similar to Adamiec et al (2010) these trap parameters were calculated following Hoogenstraten's method of measuring subtracted TL curves with variable heating rates (Table 2).

In addition to calculating lifetime at a specific temperature from estimates of trap parameters, it is possible to estimate lifetime at average burial temperature by comparing measured and known ages of a suite of samples and assuming that observed deviations are due to temperature-induced signal loss. Thiel et al. (2012) used such a technique by comparing quartz TT-OSL ages with ages derived from the 290 °C post-infrared infrared-stimulated luminescence (post-IR IRSL$_{290}$) signal from feldspars and assuming that the average burial temperature was comparable to the modern mean annual air temperature of 19 °C at their sampling site in north-eastern Tunisia. Their results suggest an average lifetime of 0.69 Ma at 19 °C (Table 1d), which is similar to lifetimes at 19 °C calculated for the medium trap of Li and Li (2006) and the Re-OSL trap of Adamiec et al. (2010) (Table 1a).

4

This paper compares natural and laboratory generated TT-OSL dose response curves to test the assumption that the response to radiation in the laboratory can be compared with the response in the natural environment. TT-OSL trap parameters E and s are calculated from laboratory measurements following Hoogenstraten's method (similar to the protocols of Adamiec et al. (2010) and Shen et al. (2011)). These parameters are used to calculate the TT-OSL signal lifetime at 10 °C. The natural lifetime of the signal at average burial temperature is calculated following the method of Thiel et al. (2012), except, in the present study, the independent age control is derived from the record of Ding et al. (2002; 'Chinese loess particle timescale' abbreviated to Chiloparts,) based on grain size variations from five stacked loess sections tuned to orbital cycles. Although the TT-OSL signal lifetime has been calculated by these two different methods in previous studies, this is the first time both measurements are made on the same samples and that the results are discussed in relation to the comparison of natural and laboratory dose response curves. The trap parameter derived lifetime estimate at modern mean annual temperature is then used to correct the measured TT-OSL ages, and the resulting corrected ages are compared against independent age control.

2 **Sample description and instrumentation**

Fine-grain (4-11 μm diameter) quartz extracts were prepared from twenty loess samples taken from the Luochuan section and from one modern analogue collected from windblown dust during fieldwork. Some of these samples (PT1, PT2, PT3, PT4, and PT5) were also used in the Chapot et al. (2012) investigation, however that study used an alternative (35-63 μm) grain size. Each of the samples in this study was treated with 10% volume to volume dilution of 37% concentrated HCl and with 20 vols H_2O_2 until no continued reactions could be identified. The samples were settled in sodium oxalate following Stokes Law to obtain 4-11 μm grain size fractions. The fine grain mineral fractions were treated with H_2SiF_6 for 14 days to remove feldspar (Roberts, 2007), and subsequently re-settled as a further quartz purification step. All of the sample preparation was undertaken in red light conditions and each of the samples passed OSL IR depletion ratio tests (Duller, 2003).

Environmental dose rates were measured with thick source alpha and beta counting using material that had been removed from the exterior of the samples. An a-value of 0.035 ± 0.003 for

5

quartz extracted from Chinese loess (Lai et al., 2008) was applied to the alpha portion of the dose rates. Gamma dose rates were calculated based on the concentrations of uranium, thorium, and potassium estimated from thick source alpha and beta counting, using the dose rate conversion factors of Guérin et al. (2011). The cosmic dose rate contribution was calculated following Prescott and Hutton (1994). Average water content during burial was assumed to be $10 \pm 5\%$ based on modern variations in soil moisture content with depth (Wang et al., 2013) and distance (Wang et al., 2012) across the Chinese Loess Plateau.

Luminescence measurements were performed on a Risø TL-DA-20 reader (Bøtter-Jensen et al., 2010) incorporating blue LEDs (470 Δ 30 nm) delivering ~45 mW/cm^2 at the sample position. The luminescence signal was recorded using an EMI9635QA photomultiplier tube with 7.5 mm of U-340 filter, and a convex quartz lens to improve signal collection efficiency (giving ~75% brighter signal). A strontium/yttrium beta source with a dose rate of circa 0.083 Gy/s was used for laboratory irradiation.

3   TT-OSL Dating Protocol

The TT-OSL dating protocol used in this study is the constant irradiation protocol of Chapot et al. (2014) (Table 3). It is a single aliquot protocol using a TT-OSL test dose signal, but maintaining the same thermal treatments and optical stimulation durations of Wang et al. (2006). To ensure removal of the TT-OSL signal before the test dose and the subsequent regenerative dose, ten TT-OSL signal cycles (260 °C 10 s preheat, 100s 125 °C OSL) are measured (Table 3, steps 6 and 12), thereby reducing the TT-OSL signal to the BT-OSL intensity. This process provides a measurement of the BT-OSL signal (tenth TT-OSL cycle, shown in red in Fig. 1) which can be subtracted from the total TT-OSL (first TT-OSL cycle, highlighted in blue in Fig. 1) to obtain a Re-OSL signal. The TT-OSL signal of each measurement cycle was defined as the luminescence recorded during the initial second of optical stimulation minus an early background from the subsequent four seconds of stimulation (Fig. 1 inset). Early background subtraction was used in order to minimize the influence of slow OSL components, which continue to decay from the initial OSL stimulation (Fig. 1).

6

4 **Natural Dose Response Curve**

The framework of independent age control provided by the Chinese Loess Plateau stratigraphy was converted into expected palaeodoses using the procedure of Chapot et al. (2012). First, the expected age for each sample was determined through linear interpolation of loess/palaeosol boundary ages from the Chiloparts record (Ding et al., 2002) with an assumed 10% error; the Chiloparts chronology was created by correlating grain size records from five loess sections, variations in the Earth's obliquity and precession, and palaeomagnetic reversals (Ding et al., 2002). Expected palaeodoses were then calculated by multiplying the expected age of each sample by its environmental dose rate (Table 4).

Six test dose normalised natural TT-OSL signals (L_n/T_n) were measured for each of the twenty one samples (165 Gy test dose, Table 3). These normalised values were plotted against expected palaeodose to construct a natural TT-OSL dose response curve (Fig. 2) describing TT-OSL signal increase with natural radiation exposure over long time scales. The results follow the expected shape of a dose response curve (signals increase with dose until plateauing at saturation) but with large scatter between aliquots for samples with low TT-OSL sensitivity (e.g. sample L9-11 with expected palaeodose of ~3500 Gy). The natural TT-OSL dose response curve constructed in this study is best described by a double saturating exponential function with D_0 values of 1300 and 110 Gy.

Determining a reliable maximum limit to the estimation of equivalent doses based on the shape of the corresponding dose response curve is problematic, but a pragmatic value of $2D_0$ has been previously suggested (e.g. Wintle and Murray, 2006). This value cannot be calculated for dose response curves fitted with more than a single exponential component, such as the natural TT-OSL dose response curve measured in this study. However, Wintle and Murray (2006) noted that $2D_0$ occurs when the OSL signal is about 15% below the saturation value of the dose response curve. Therefore, in this study, the prudent maximum limit of the technique was approximated by the dose corresponding to the signal intensity (L_x/T_x) that is 15% below the signal intensity at saturation (determined by summing the I_{max} values of the two saturating exponential components). For the natural TT-OSL dose response curve, this value is ~ 2200 Gy. If the natural TT-OSL DRC is fitted

7

with a single saturating exponential, the curve does not describe the data well for doses less than 500 Gy, however, the corresponding $2D_0$ value is ~1950 Gy.

5   SAR Dose Response Curves

Twenty one single aliquot regenerative (SAR) laboratory TT-OSL dose response curves (DRCs) were constructed using one aliquot from each of the twenty one samples and following the protocol shown in Table 3 (165 Gy test dose). Four examples of individual SAR TT-OSL DRCs are shown in subfigures 3a-3d, including the modern analogue sample (Fig. 3a), a bright aliquot (Fig. 3b), a dim aliquot (Fig. 3c), and the oldest sample (Fig. 3d). Subfigure 3e shows all twenty-one SAR TT-OSL DRCs, an average SAR TT-OSL DRC (fit to all the data) and the natural TT-OSL DRC. The data for the natural DRC shown in figure 2 depicts L_n/T_n values measured for each aliquot, but in subfigure 3e, the L_n/T_n values for each sample have been averaged to a central value with standard error.

The average TT-OSL laboratory dose response curve can be equally well described by a single or double saturating exponential with a saturation dose similar to the natural TT-OSL dose response curve ($2D_0$ of 2700 Gy for single saturating exponential fit, D_0 values of 1500 and 150 Gy for double saturating exponential fit). However, the regenerated laboratory doses had much brighter signals relative to the subsequent test dose, resulting in deviation between natural and laboratory TT-OSL dose response curves at circa 150 Gy (Fig. 3). This deviation causes TT-OSL equivalent doses >150 Gy to increase in stratigraphic order but increasingly underestimate the palaeodose (true burial dose).

In order to test that the difference between the natural and laboratory TT-OSL DRCs was not caused by uncorrected sensitivity change during the intensive TT-OSL dating protocol (see protocol, Table 3), laboratory doses ranging from 0 to ~3500 Gy were added to untreated aliquots of the modern sample (JYM) and the resulting L_x/T_x ratios (red stars, Fig. 3a and 3e) were compared with the L_x/T_x values of other dose response curves generated in this study. Subfigure 3a compares the L_x/T_x ratios of these additive doses (red stars) with a SAR laboratory dose response curve generated

8

using a different aliquot of the same sample (white circles). The excellent agreement observed (Fig. 3a) suggests that minimal uncorrected sensitivity change occurred during the TT-OSL SAR protocol.

When the additive doses (red stars) are compared against the average Luochuan SAR laboratory dose response curve (solid black line, Fig. 3e), the L_x/T_x ratios are in agreement up to 745 Gy, but higher additive doses have L_x/T_x ratios lower than the average curve, suggesting that the modern dust sample (JYM) may have slight differences in dose response curve shape compared to the loess samples. Finally, when the additive doses (red stars) are compared with the natural TT-OSL dose response curve (dashed black line) it can be observed that the L_x/T_x ratios deviate at ~150 Gy, similar to the other laboratory dose response curves. These results suggest that the deviation between natural and laboratory dose response curves is not related to sensitivity change during measurement of the natural TT-OSL signal.

6 **TT-OSL trap parameters**

One potential explanation for the deviation between the natural and laboratory dose response curves is poor thermal stability of the natural luminescence signal at environmental burial temperatures. If the average duration of time that an electron will reside in a specific trap at a specific temperature before being thermally evicted (trap lifetime, τ) is too short, a significant proportion of the trapped electrons will be evicted during the sample's age span, resulting in lower than expected L_n values when the natural luminescence signal is measured. For a sample held at constant temperature, the average lifetime (τ) of an electron in a specific trap can be calculated by equation 1:

$$\tau = s^{-1} \exp\left(\frac{E}{kT}\right) \qquad \text{Eqn. 1}$$

Where s is the frequency factor (s^{-1}), E is the trap depth (eV), T is temperature (K) and k is Boltzmann's constant (eV/K). Estimation of the natural burial lifetime of a given trap therefore requires characterisation of the trap parameters E and s, as well as an estimate of the average burial temperature. For this study, the average burial temperature was assumed to be similar to the modern mean annual air temperature (10 °C, Hu et al. 2015), and E and s values were calculated using Hoogenstraten's method on subtracted TL peaks for one pre-sensitised aliquot each of five samples

9

(PT1, PT2, PT3, PT4, PT5) (aliquots that had previously experienced numerous cycles of heating and irradiation until sensitivity changes became minimal). The TL glow curve of each aliquot was measured at different heating rates to determine the charge trapped before TT-OSL stimulation (Fig. 4a, Table 2, TLa) and the charge remaining after TT-OSL stimulation (Fig. 4b, Table 2, TLb). Then, to determine the thermoluminescence that was depleted during the TT-OSL stimulation, the post-stimulation TL curve (TLb) was subtracted from the pre-stimulation glow curve (TLa) of the same heating rate (Fig. 4d). This experiment is similar to the trap characterisation protocols of Adamiec et al. (2010) and Shen et al. (2011) which also use Hoogenstraten's method on subtracted TL curves (Table 2).

The loss of TL signal observed when the TT-OSL signal is measured, as obtained by the subtraction method used in this study (Table 2), is a relatively low intensity signal dominated by a broad TL peak centred at ~290 °C (5 °C/s) with some contributions from higher TL peaks (Fig. 4d, lighter-coloured line). However an additional experiment comparing the TL signal removed by the TT-OSL protocol (260 °C 10 s, OSL 125 °C 300 s, 260 °C 10 s, OSL 125 °C 100 s) with the TL signal removed by continuous OSL stimulation without the thermal transfer preheat step (260 °C 10 s, OSL 125 °C 400 s; Fig. 4c) demonstrates that the contributions from higher TL peaks are due to the OSL slow components and that the TL origin of the TT-OSL signal is only the primary peak (centred at ~290 °C in Fig. 4d).

Calculation of E and s values using Hoogenstraten's method requires that the temperature (T_m) corresponding to peak signal intensity (I_0) be identified. This identification is critical and can significantly affect the kinetic parameter values that are calculated. Previous researchers have suggested that T_m can be identified within ±2 °C based on close visual inspection of the TL curves (Shen et al., 2011). In order to avoid subjective bias, T_m was identified in this study as the temperature corresponding to the maximum signal intensity of data smoothed with a 50 °C moving average (Fig. 5), though I_0 was measured from the unmodified data.

The heating rate (β) and T_m of each curve were used to calculate values of $1/kT_m$ and $\ln(T_m^2/\beta)$, which were then fit with a linear regression (Fig. 6) following the method and equations of Adamiec et al. (2010, Eqn. 1 therein). The slope of the fitted line is an estimation of trap depth (E) in

eV. Calculation of the frequency factor is less straightforward. Based partly on extrapolating the linear regression to the y-axis, frequency factor calculations also require a correction for thermal quenching. Thermal quenching estimates (W) were calculated based on mathematical fitting of the relationship between I_0 and T_m, following the method and equations of Adamiec et al. (2010, Eqn. 3 therein) (Fig. 7). However, W values calculated in this manner (W = 0.20 – 0.33 eV; Table 1b) are lower than previously published measurements for TT-OSL (Adamiec et al., 2010; ReOSL W = 0.48 and BT-OSL W = 0.56 eV) and for quartz in general (e.g. Subedi et al., 2011; W = 0.65 ± 0.03 eV).

Shen et al. (2011) reported an inability to accurately measure W values using this method because of sensitivity change during the TL measurements. Instead, they measured W values for their samples by varying the optical bleaching temperature and obtained a value of 0.70 ± 0.03 eV, in agreement with previous measurements for quartz. In the present study, s values were calculated using both W values estimated during the experiment and the 0.65 ± 0.03 eV value recommended for quartz by Subedi et al. (2011). In addition to calculating the trap parameters for each of the five tested samples individually, the parameters were also calculated by fitting all the data combined and sample-specific values were integrated by weighted averaging in order to provide an estimate of general TT-OSL signal lifetimes for the field-site.

The resulting TT-OSL trap parameters and associated lifetimes at 10 °C are listed in sub-tables 1b and 1c. Trap depth values calculated for the different samples are consistent within uncertainties, but frequency factor estimates are more varied. Applying the thermal quenching values obtained from previous studies (W = 0.65 ± 0.03 eV) increases the calculated expected signal lifetime at 10 °C by tens of thousands of years. Weighted averages of the E, s, W, and τ values are within error of estimates obtained by fitting the combined data. Average lifetime estimates were calculated by averaging the sample specific lifetime estimates and not by calculating lifetime from the averaged E and s values, which would have resulted in lower estimates. The values calculated by fitting the combined data of the different samples and assuming similar thermal quenching to previous studies are also compared with the values reported by Shen et al. (2011), Adamiec et al. (2010), and Li and Li (2006) in table 1.

The difficulties of signal lifetime estimates calculated in this manner (e.g. parameter dependence on T_m identification, sensitivity changes affecting thermal quenching estimates, long extrapolation necessary for calculating s) and the less than certain correlation of the TL signal loss with the TT-OSL signal that is measured (Arnold and Demuro, in press), can reduce one's confidence in the accuracy of laboratory determinations of signal lifetime. It is therefore critical that, when possible, laboratory lifetime estimates be compared to approximations of the natural signal lifetime during burial, which can be calculated by comparing measured and expected ages.

7 **Natural signal lifetime**

Thiel et al. (2012) compared TT-OSL ages to post-IR IRSL$_{290}$ ages and calculated a field estimate of the lifetime of the TT-OSL signal by assuming that the post-IR IRSL$_{290}$ ages were accurate and that the 19 °C modern mean annual air temperature is a reasonable approximation of the average burial temperature. Their results suggested a natural TT-OSL signal lifetime of 0.69 Ma which is consistent with lifetime estimates for the TT-OSL signal at 19 °C calculated from the trap parameters of Li and Li (2006) and Adamiec et al. (2010) (Table 1a).

Similar calculations can be made in this study using the Chiloparts chronology (Ding et al., 2002) and assuming an average burial temperature of 10 °C (approximate to the modern mean annual air temperature (Hu et al., 2015)). TT-OSL equivalent doses for each of the samples were calculated by determining the L_n/T_n value of the natural dose response curve (dashed line, Fig. 3e) corresponding to the sample's expected palaeodose and interpolating that L_n/T_n value onto the average SAR laboratory dose response curve (Fig. 3e). Sample ages were then calculated by dividing the equivalent doses by the sample specific dose rates. Ages calculated in this manner are based directly on the difference between the natural and laboratory dose response curves. Measured TT-OSL ages are plotted against expected ages in figure 8 and these datapoints can be fit with the following equation that includes average burial temperature (*t*) and signal lifetime (τ) as parameters:

$$f = \left(\left(\frac{\tau}{t}\right) * \left(1 - \exp\left(-\frac{t}{\tau}\right)\right)\right) * t \qquad \text{Eqn. 2}$$

The measured and expected ages of all the samples were fit with equation 2 and the resulting function is shown on figure 8 as 'Fit to all Data. This same fitting procedure was also used for only the subset of samples (Data 1) with L_n/T_n values below the estimated maximum limit of reliability for the natural dose response curve (2200 Gy) and the results are shown on figure 8 as 'Fit to Data 1'. The signal lifetime at 10 °C calculated using the E and s values for the combined data and the thermal quenching value (W) of Subedi et al. (2011; 0.65 ± 0.03 eV), as discussed in section 6, was used to define a similar function that is plotted on figure 8 as 'Lifetime at 10 °C' ($\tau = 180$ ka, Table 1c). Lifetime estimates obtained by fitting equation 2 to the data are 203 ± 5 ka for all the samples and 175 ± 5 ka for the subset of samples with L_n/T_n values less than 2200 Gy. These estimates are consistent with lifetimes calculated from trap parameters in this study and Shen et al. (2011), but are more than an order of magnitude lower than the lifetimes suggested by Li and Li (2006), Adamiec et al. (2010), and Thiel et al. (2012).

Mathematical functions described by equation 2 (e.g. fitted lines in Fig. 8) have an asymptote at old ages suggesting that if the deviation between natural and laboratory dose response curves is caused by poor thermal stability, there is a maximum limit to TT-OSL ages that can be generated in a laboratory. In figure 8, this limit occurs at about 200 ka, suggesting that even an infinitely old sample would not have a laboratory TT-OSL age >200 ka, unless the sample's thermal stability or average burial temperature was significantly different to the other samples in the study. However, TT-OSL ages >200 ka have been reported in several studies (e.g. Duller et al., 2015 and Thiel et al., 2012) , including a previous study at Luochuan (Wang et al., 2006), which calculated a (constant-irradiation) TT-OSL age of ~475 ka for a sample taken near the Brunhes-Matayuma palaeomagnetic boundary. Perhaps differences in the maximum TT-OSL age that can be measured in a laboratory highlight variability in TT-OSL signal thermal stability and could be a useful measure for estimating thermal stability in future studies.

8 Discussion

The late saturation of the natural TT-OSL dose response curve suggests that the signal could be used to extend the age range up to the ~2200 Gy limit of the natural TT-OSL dose response

curve if differences between natural and laboratory DRCs can be eliminated or corrected for. General agreement of field and laboratory measurements of the TT-OSL signal lifetime demonstrated in this study suggest the possibility of correcting TT-OSL ages for signal loss during burial based on laboratory measurements of thermal stability. This possibility was investigated by using the inverse of equation 2 and the trap parameter derived lifetime estimate ($\tau = 180 \pm 10$ ka) to correct the TT-OSL ages obtained in this study (Fig. 9, Cor-1). Sample specific thermal stability corrections based on sample specific laboratory thermal stability measurements (Table 1c) for a subset of samples are also shown in figure 9 (Cor-2).

Lifetime-corrected TT-OSL ages are within error of the expected ages with the exception of the sample-specific correction for some samples. Thermal stability corrected TT-OSL ages generated in this manner can accurately date older samples but have poor precision due to both the low signal intensity and kinetic parameter measurement difficulties. The poor accuracy of some of the sample-specific corrected ages may reflect the difficulty of the laboratory lifetime measurements and the need for measurements from multiple aliquots. In this study, the laboratory thermal stability measurements that were in closest agreement to the apparent natural lifetime were generated by fitting data extracted from subtracted TL signals of multiple samples, but this could be an effect of the natural lifetime also being calculated by averaging signals from multiple samples.

Correction of TT-OSL ages for signal lifetime has been previously applied (Duller et al., 2015; Ryb et al., 2013) using the signal lifetime values reported by Adamiec et al. (2010). However, significant differences in TT-OSL signal lifetime calculated by Li and Li (2006), Adamiec et al. (2010), and Thiel et al. (2012) (~4 Ma at 10 °C) and by Shen et al (2011) and this study (~200 ka at 10 °C) suggests that TT-OSL thermal stability may vary between samples or study regions. In addition to inherent signal lifetime variability and measurement difficulty, the sensitivity of signal lifetime corrected TT-OSL ages to fluctuations in burial temperature remains to be investigated in further detail (Duller et al., 2015).

Although there may be other factors influencing the agreement between natural and laboratory TT-OSL dose response curves (and hence the maximum age range of TT-OSL dating), the data from this study suggests that thermal instability of the TT-OSL signal could account for the

majority of the observed deviation, and that differences are unlikely to be caused by sensitivity change during measurement of the natural TT-OSL signal.

9 **Conclusions**

This study compared natural and laboratory generated thermally transferred optically stimulated luminescence (TT-OSL) dose response curves (DRCs) for fine-grain quartz extracts from the Luochuan loess section in central China. The natural TT-OSL DRC saturates at about 2200 Gy, much later than the fast component OSL signal, but deviates from the laboratory TT-OSL DRC at circa 150 Gy resulting in TT-OSL equivalent dose underestimation. Comparison of TT-OSL signal lifetime calculated from measurement-derived values of trap parameters and the natural lifetime of the TT-OSL signal at average burial temperature, suggests this deviation is primarily due to thermal instability. The agreement of these two independent assessments of TT-OSL signal lifetime at Luochuan suggests that laboratory measurements of thermal stability reflect burial lifetimes in nature, and can potentially be used to correct for the difference between natural and laboratory dose response curves. This technique could enable the TT-OSL signal to extend the age range of quartz luminescence dating up to the saturation level of the natural TT-OSL dose response curve.

References

Adamiec, G., Duller, G.A.T., Roberts, H.M., Wintle, A.G., 2010. Improving the TT-OSL SAR protocol through source trap characterisation. Radiat Meas 45, 768-777.

Arnold, L.J., Demuro, M., in press. Insights into TT-OSL signal stability from single-grain analyses of known-age deposits at Atapuerca, Spain. Quat. Geochron.

Arnold, L.J., Demuro, M., Parés, J.P., Pérez-González, A., Arsuaga, J.L., Bermúdez de Castro, J.M., Carbonell, E., in press. Evaluating the suitability of extended-range luminescence dating techniques over early and Middle Pleistocene timescales: Published datasets and case studies from Atapuerca, Spain. Quat International

Bailey, R.M., 2004. Paper I- simulation of dose absorption in quartz over geological timescales and its implications for the precision and accuracy of optical dating. Radiat Meas 38, 299-310.

Bøtter-Jensen, L., Thomsen, K.J., Jain, M., 2010. Review of optically stimulated luminescence (OSL) instrumental developments for retrospective dosimetry. Radiat Meas 45, 253-257.

Buylaert, J.P., Vandenberghe, D., Murray, A.S., Huot, S., De Corte, F., Van den Haute, P., 2007. Luminescence dating of old (>70 ka) Chinese loess: A comparison of single-aliquot OSL and IRSL techniques. Quat Geochronol 2, 9-14.

Chapot, M.S., Roberts, H.M., Duller, G.A.T., Lai, Z.P., 2012. A comparison of natural- and laboratory-generated dose response curves for quartz optically stimulated luminescence signals from Chinese Loess. Radiat Meas 47, 1045-1052.

Chapot, M.S., Duller, G.A.T., Roberts, H.M., 2014. Assessing the impact of pulsed-irradiation procedures on the thermally transferred OSL signal in quartz. Radiat Meas 65, 1-7.

Ding, Z. L., Derbyshire, E., Yang, S. L., Yu, Z. W., Xiong, S. F., Liu, T. S., 2002. Stacked 2.6-Ma grain size record from the Chinese loess based on five sections and correlation with the deep-sea δ18O record. Paleoceanography 17, 1-21.

Duller, G.A.T., 2003. Distinguishing quartz and feldspar in single grain luminescence measurements. Radiat Meas 37, 161-165.

Duller, G.A.T., Wintle, A.G., 2012. A review of the thermally transferred optically stimulated luminescence signal from quartz for dating sediments. Quat Geochronol 7, 6-20.

Duller, G.A.T., Tooth, S., Barham, L., Tsukamoto, S. 2015. New archaeological investigations at Kalambo Falls, Zambia: Luminescence chronology and site formation. Journal of Human Evolution 85: 111-125..

Guérin, G., Mercier, N., Adamiec, G., 2011. Dose-rate conversion factors: update. Ancient TL 29, 5-8.

Hu, P., Liu, Q., Heslop, D., Roberts, A.P., Jin, C., 2015. Soil moisture balance and magnetic enhancement in loess–paleosol sequences from the Tibetan Plateau and Chinese Loess Plateau. Earth and Planetary Science Letters 409, 120-132.

Lai, Z.P., Zöller, L., Fuchs, M., Brückner, H., 2008. Alpha efficiency determination for OSL of quartz extracted from Chinese loess. Radiat Meas 43, 767-770.

Lai, Z.P., 2010. Chronology and the upper dating limit for loess samples from Luochuan section in the Chinese Loess Plateau using quartz OSL SAR protocol. Journal of Asian Earth Sciences 37, 176-185.

Li, B., Li, S.H., 2006. Studies of thermal stability of charges associated with thermal transfer of OSL from quartz. J. Phys. D: Appl. Phys. 39, 2941-2949.

Pickering, R., Jacobs, Z., Herries, A.I.R., Karkanas, P., Bar-Matthews, M., Woodhead, J.D., Kappen, P., Fisher, E., Marean, C.W., 2013. Paleoanthropologically significant South African sea caves dated to 1.0 million years using a combination of U-Pb, TT-OSL and palaeomagnetism. Quat Sci Rev 65, 39-52.

Prescott. J.R., Hutton, J.T., 1994. Cosmic ray contributions to dose rates for luminescence and ESR dating: Large depths and long-term time variations. Radiat Meas 23, 497-500.

Roberts, H.M., 2007. Assessing the effectiveness of the double-SAR protocol in isolating a luminescence signal dominated by quartz. Radiat Meas 42, 1627-1636.

Ryb, U., Matmon, A., Porat, N., Katz, O., 2013. From mass-wasting to slope stabilization – putting constrains on a tectonically induced transition in slope erosion mode: a case study in the Judea Hills, Israel. Earth Surface Processes and Landforms 38, 551-560.

Shen, Z.X., Mauz, B., Lang, A., 2011. Source-trap characterization of thermally-transferred OSL in quartz. J. Phys. D: Appl. Phys. 44, 295405.

Subedi, B., Oniya, E., Polymeris, G.S., Afouxenidis, D., Tsirliganis, N.C., Kitis, G., 2011. Thermal quenching of thermoluminescence in quartz samples of various origin. Nucl. Instrum. Methods Phys. Res. B 269, 572-581.

Thiel, C., Buylaert, J.-P., Murray, A.S., Elmejdoub, N., Jedoui, Y., 2012. A comparison of TT-OSL and post-IR IRSL dating of coastal deposits on Cap Bon peninsula, north-eastern Tunisia. Quat Geochronol. 10, 209-217.

Wang, X.L., Lu, Y.C., Wintle, A.G., 2006. Recuperated OSL dating of fine-grained quartz in Chinese loess. Quat Geochronol 1, 89-100.

Wang, Y., Shao, M., Liu, Z., Warrington, D.N., 2012. Regional spatial pattern of deep soil water content and its influencing factors. Hydrological Sciences Journal 57, 265-281.

Wang, Y., Shao, M., Liu, Z., 2013. Vertical distribution and influencing factors of soil water content within 21-m profile on the Chinese Loess Plateau. Geoderma 193-194, 300-310.

Figure Captions

1. Signal intensities of the OSL and TT-OSL signals for an aliquot of sample PT5 in response to a dose of 165 Gy. The first decay is the 300 s OSL signal. The TT-OSL signal was defined by subtracting the early background subtracted tenth TT-OSL cycle (red) from the early background subtracted first TT-OSL cycle (blue). Signals are separated by heating to 260 °C for 10 s.

2. Natural TT-OSL dose response curve. Each point represents a L_n/T_n measurement from a single aliquot plotted against the sample's expected palaeodose. The data are fitted with a double saturating exponential function of the form: $L_n/T_n (D) = 3.4*(1-exp(-D/1300)) + 0.7*(1-exp(-D/110)) + 0.0$.

3. Laboratory dose response curves measured in this study are shown as grey lines with individual L_x/T_x measurements represented by white circles. Subfigures a-d show SAR dose response curves for individual aliquots of a) the modern sample b) a bright aliquot c) a dim aliquot and d) the oldest sample. First TT-OSL signal response to the natural test dose for these aliquots is shown in corner insets. Subfigure e) compares laboratory and natural dose response curves. The natural dose response curve is the same as in figure 2, but L_n/T_n values have been averaged by sample with error bars depicting standard error. L_x/T_x values of additive laboratory doses administered to untreated aliquots of the modern sample are shown in red on subfigures a) and e).

4. TL glow curves for sample PT5 measured with a 5 °C/s heating rate following a 2100 Gy dose. Subfigure a) shows the U340 TL signal remaining after a 10 s 260 °C preheat and a 300 s 125 °C blue optical stimulation (TLa). Subfigure b) shows the U340 TL signal remaining after the same treatment and a TT-OSL cycle (TLb). The TL signal removed during the TT-OSL cycle is obtained by subtracting TLb from TLa and is shown in dark blue on subfigure d). Subfigure c) shows the U340 TL signal remaining after a 10 s 260 °C preheat and a 400 s 125 °C blue optical stimulation (TLc). Subtracting TLb from the TLc signal demonstrates the TL signal removed during the TT-OSL cycle due to the thermal transfer preheat, shown in light blue on subfigure d). The difference between the light and dark blue signals on subfigure d) is interpreted to be the TL signal removed by slow blue OSL components.

5. a) TL glow curve for sample PT5 measured with a 0.05 °C/s heating rate as well as the 50 °C moving averaged signal that was used to identify the temperature corresponding to the initial TL peak. b) TL glow curves for sample PT5 measured with varying heating rates from 0.05 to 5.00 °C/s.

6. a) Data derived from TL peak temperatures and heating rates of sample PT5 fit with a linear regression to identify the TT-OSL trap depth. The error bars represent ± 2°C uncertainty in peak temperature. b) Data derived from TL peak temperatures and heating rates of all five samples measured, the combined data are fit with a linear regression to identify the general (non-sample-specific) TT-OSL trap depth.

7. a) Initial TL peak intensity vs peak temperature with ± 2°C uncertainty for each of the PT5 TL glow curves, fitted to obtain an estimate of thermal quenching. b) Initial TL peak intensities vs peak temperatures for all five samples measured. Thermal quenching values calculated with this method were lower than previously published values for quartz and were not always used in further calculations in this study, see text for details.

8. Expected and measured ages are compared and shown to deviate from the 1:1 line after 45 ka. Field estimates of signal lifetime were obtained by fitting equation 2 to either all the data (Black dotted line) or the data subset with unsaturated natural signals (Fit to Data 1). TT-OSL signal lifetime at 10 °C, as calculated from laboratory thermal stability measurements (all samples combined, assumed 0.65 eV thermal quenching), is shown by a dotted grey line.

9. Comparison of lifetime corrected TT-OSL ages against measured and expected ages. The red squares (Cor-1) represent TT-OSL ages corrected by the general lifetime of the five PT samples (all samples combined, assumed 0.65 eV thermal quenching), while the purple triangles (Cor-2) represent TT-OSL ages corrected by sample-specific lifetimes. Error bars that continue beyond the scale of the plot are infinite and any missing datapoints are due to corrected ages of infinity.

Table Captions

1. Table 1: Comparison of TT-OSL kinetic parameters (E and s), thermal quenching (W), and signal lifetimes from this and other studies. T1a) Previously published values. T1b) Values calculated in this study using individual sample estimates of thermal quenching. T1c) Values calculated in this study assuming thermal quenching of W = 0.65 eV. T1d) Estimates of field-lifetime based on comparing known and expected ages and assuming burial temperature similar to modern annual air temperature.
2. Comparison of protocols used for estimating TT-OSL thermal stability
3. TT-OSL dating protocol used in this study
4. Dose rates and expected palaeodoses for the samples analysed in this study

A. Reference	Trap	E (eV)	s (x 10^{10} s^{-1})	W (eV)	τ_{10} (Ma)	τ_{19} (Ma)
Li and Li 2006	Medium	1.14 ± 0.05	0.00017*	-	3.7	0.89
Adamiec et al. 2010	Re-OSL	1.46	76	0.52 (0.48)	4.5	0.71
Shen et al. 2011	Trap A	1.34 ± 0.05	9.5	0.70 ± 0.03	0.24	0.05

B. Sample	Trap	E (eV)	s (x 10^{10} s^{-1})	W (eV)	τ_{10} (Ma)	τ_{19} (Ma)
PT1	TT-OSL	1.32 ± 0.09	9.5 ± 1.6	0.28 ± 0.09	0.09 ± 0.02	0.02 ± 0.00
PT2	TT-OSL	1.32 ± 0.05	10.7 ± 1.5	0.27 ± 0.09	0.10 ± 0.01	0.02 ± 0.00
PT3	TT-OSL	1.37 ± 0.05	31.4 ± 2.6	0.25 ± 0.04	0.24 ± 0.02	0.04 ± 0.00
PT4	TT-OSL	1.30 ± 0.05	7.1 ± 0.5	0.20 ± 0.03	0.07 ± 0.00	0.01 ± 0.00
PT5	TT-OSL	1.35 ± 0.05	17.8 ± 2.9	0.33 ± 0.11	0.17 ± 0.03	0.03 ± 0.00
Combined	TT-OSL	$\mathbf{1.33 \pm 0.03}$	$\mathbf{13.0 \pm 0.9}$	$\mathbf{0.27 \pm 0.04}$	$\mathbf{0.12 \pm 0.01}$	$\mathbf{0.02 \pm 0.00}$
Average	TT-OSL	$\mathbf{1.33 \pm 0.02}$	$\mathbf{20.0 \pm 9.6}$	$\mathbf{0.27 \pm 0.05}$	$\mathbf{0.16 \pm 0.06}$	$\mathbf{0.02 \pm 0.01}$

C. Sample	Trap	E (eV)	s (x 10^{10} s^{-1})	W (eV)	τ_{10} (Ma)	τ_{19} (Ma)
PT1	TT-OSL	1.32 ± 0.09	6.1 ± 1.1	0.65 ± 0.03	0.14 ± 0.02	0.03 ± 0.00
PT2	TT-OSL	1.32 ± 0.05	6.9 ± 0.9	0.65 ± 0.03	0.16 ± 0.02	0.03 ± 0.01
PT3	TT-OSL	1.37 ± 0.05	20.2 ± 2.4	0.65 ± 0.03	0.38 ± 0.04	0.07 ± 0.01
PT4	TT-OSL	1.30 ± 0.05	4.2 ± 0.5	0.65 ± 0.03	0.12 ± 0.02	0.02 ± 0.00
PT5	TT-OSL	1.35 ± 0.05	12.2 ± 1.5	0.65 ± 0.03	0.25 ± 0.03	0.05 ± 0.01
Combined	TT-OSL	$\mathbf{1.33 \pm 0.03}$	$\mathbf{8.4 \pm 0.7}$	$\mathbf{0.65 \pm 0.03}$	$\mathbf{0.18 \pm 0.01}$	$\mathbf{0.03 \pm 0.00}$
Average	TT-OSL	$\mathbf{1.33 \pm 0.02}$	$\mathbf{12.7 \pm 6.3}$	$\mathbf{0.65 \pm 0.03}$	$\mathbf{0.24 \pm 0.10}$	$\mathbf{0.04 \pm 0.02}$

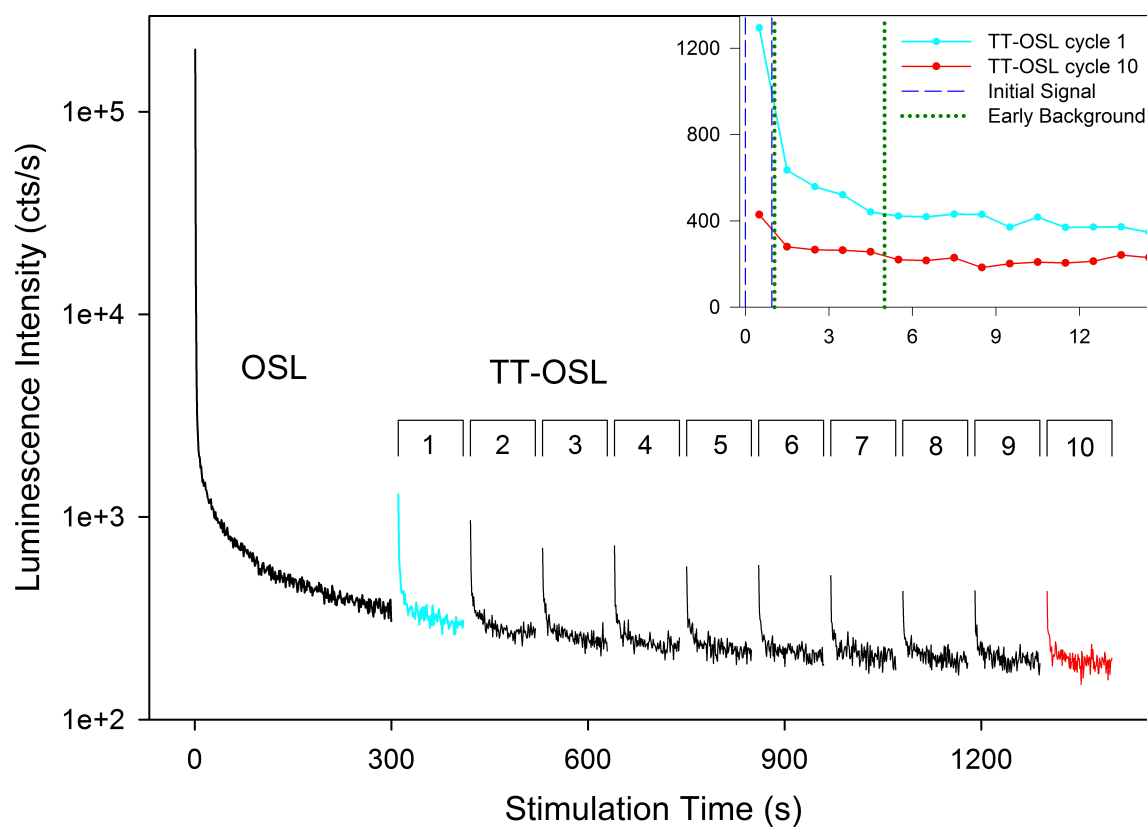| D. Reference	Trap				τ_{10} (Ma)	τ_{19} (Ma)
This study	Re-OSL	-	-	-	0.175 ± 0.005	-
Thiel et al. 2012	TT-OSL	-	-	-	-	0.69

*s value as calculated from reported values for lifetime and trap depth, this value is $10^{6.23}$ but is rounded to $10^{6.2}$ in the original paper
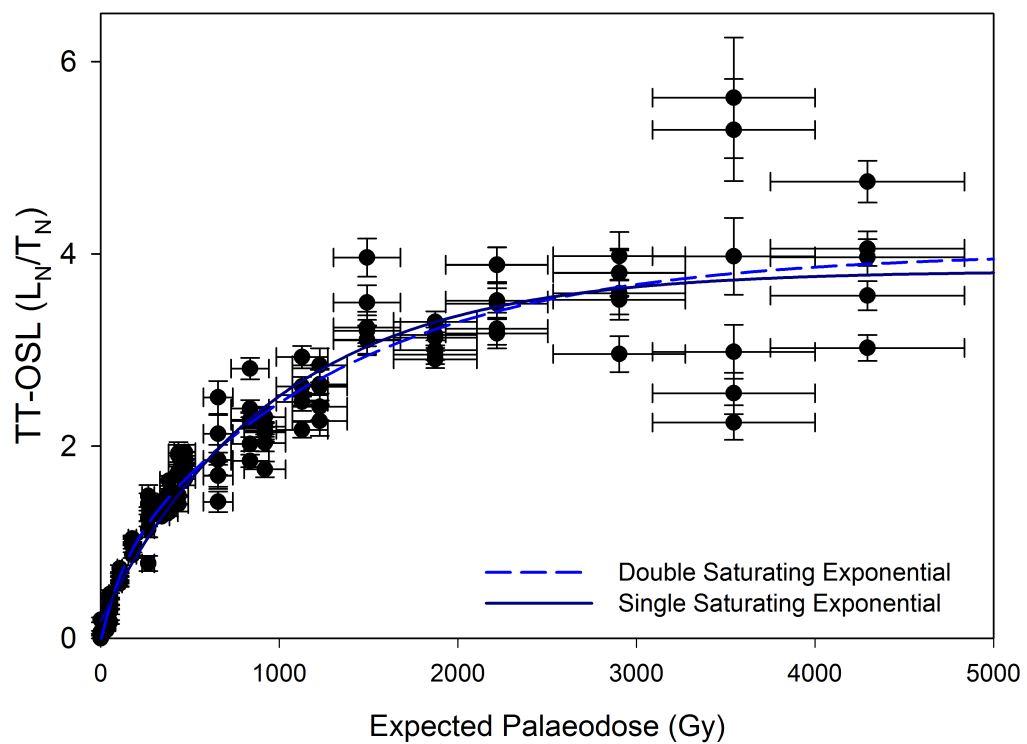
Step	Li and Li 2006 One aliquot per T	Adamiec et al 2010: ReOSL = TTOSL-BTOSL TT-OSL	BT-OSL	Shen et al 2011: Trap A = TL2-TL3 TL2	TL3	This Study: TT-OSL = TLa-TLb TLa	TLb
1	Natural Dose (~270 Gy)	TL 450 °C at 5 °C/s	TL 450 °C at 5 °C/s	TL 450 °C at 5 °C/s	TL 450 °C at 5 °C/s	TL 450 °C at 5 °C/s	TL 450 °C at 5 °C/s
2	OSL 160 °C/ 4000 s	360 Gy Dose	360 Gy Dose	57.6 Gy Dose	57.6 Gy Dose	2100 Gy Dose	2100 Gy Dose
3	TL T °C (260 - 340) for t s	Preheat 260 °C/ 10 s	Preheat 260 °C/ 10 s	Preheat 260 °C/ 10 s	Preheat 260 °C/ 10 s	Preheat 260 °C/ 10 s	Preheat 260 °C/ 10 s
4	OSL 160 °C/ 2000 s	LM-OSL 125 °C/ 80 s	LM-OSL 125 °C/ 80 s	OSL 125 °C/ 40 s	OSL 125 °C/ 40 s	OSL 125 °C/ 300 s	OSL 125 °C/ 300 s
5	TL T °C (260 - 340) for 10 s	TL 450 °C at X °C/s **(TTOSL)**	OSL 310 °C/ 40 s	TL 450 °C at X °C/s **(TL2)**	Preheat 300 °C/ 10 s	TL 450 °C at X °C/s **(TLa)**	Preheat 260 °C/ 10 s
6	OSL 160 °C/ 2000 s **(L$_x$)**		TL 450 °C at X °C/s **(BTOSL)**		OSL 125 °C/ 40 s		OSL 125 °C/ 100 s
7	Repeat from Step 2				TL 450 °C at X °C/s **(TL3)**		TL 450 °C at X °C/s **(TLb)**
	with increased t						
8				Test Dose	Test Dose		
9				Preheat 220 °C/ 10 s	Preheat 220 °C/ 10 s		
10				OSL 125 °C/ 40 s	OSL 125 °C/ 40 s		

Step	Dating Protocol
1	Dose (or Natural)
2	Preheat 260 °C/ 10 s
3	OSL 125 °C/ 300 s
4	Preheat 260 °C/ 10 s
5	OSL 125 °C/ 100 s **(L_x)**
6	Repeat Steps 4-5 nine times
7	165 Gy Test Dose
8	Preheat 260 °C/ 10 s
9	OSL 125 °C/ 300 s
10	Preheat 260 °C/ 10 s
11	OSL 125 °C/ 100 s **(T_x)**
12	Repeat Steps 10-11 nine times

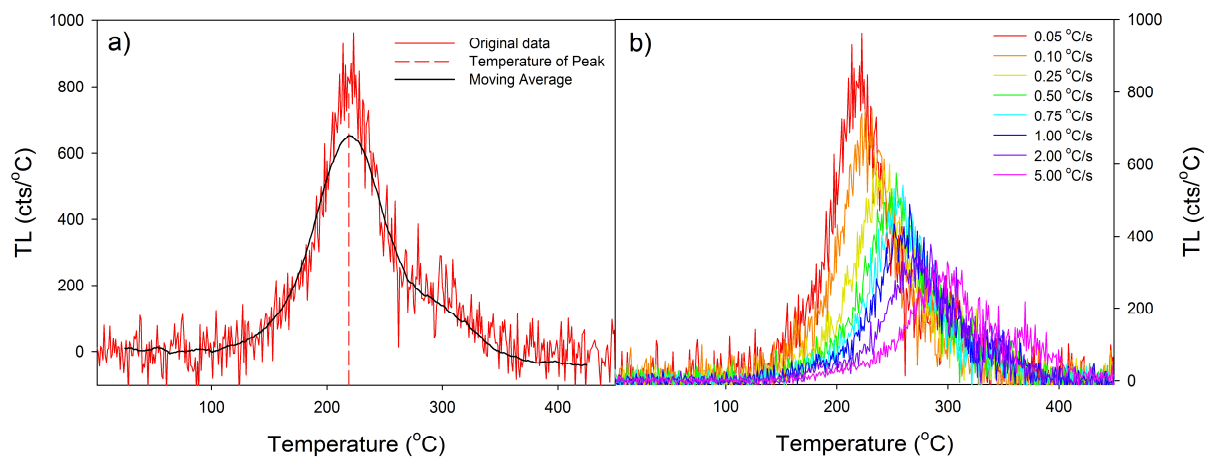| Sample	Depth (m)	Dose Rate (Gy/ka)	Exp. Age (ka)	Exp. Palaeodose (Gy)
JYM	0.0	-	0 ± 0	0 ± 0
S0 Lower - 11	1.1	3.94 ± 0.32	8 ± 1	32 ± 4
LC0.0	2.0	3.59 ± 0.26	15 ± 1	52 ± 6
LC2.0	4.0	4.04 ± 0.29	26 ± 3	106 ± 13
LC4.5	6.5	3.91 ± 0.29	45 ± 5	177 ± 22
LC7.5	9.5	3.73 ± 0.29	71 ± 7	266 ± 34
LC8.0	10.0	4.28 ± 0.34	80 ± 8	341 ± 44
LC9.0	11.0	3.87 ± 0.32	99 ± 10	382 ± 50
LC10.5	12.5	3.69 ± 0.28	128 ± 13	471 ± 59
PT1*	12.7	3.29 ± 0.26	132 ± 13	434 ± 55
LC13.5	15.5	3.86 ± 0.29	170 ± 17	657 ± 82
LC17.5	19.5	3.83 ± 0.29	240 ± 24	919 ± 116
PT2*	20.3	3.31 ± 0.26	252 ± 25	835 ± 106
L3-11	22.8	3.75 ± 0.30	301 ± 30	1127 ± 144
PT3*	25.8	3.62 ± 0.27	339 ± 34	1226 ± 153
PT4*	31.9	3.53 ± 0.27	422 ± 42	1490 ± 187
L5-11	34.4	3.81 ± 0.28	491 ± 49	1873 ± 233
PT5*	40.4	3.55 ± 0.29	624 ± 62	2218 ± 287
L8-11	51.3	3.61 ± 0.29	805 ± 81	2904 ± 370
L9-11	62.4	3.70 ± 0.30	959 ± 96	3545 ± 455
L10-11	65.3	4.21 ± 0.33	1020 ± 102	4294 ± 543

*These PT samples are the same PT samples investigated by Chapot et al. 2012 but are a finer grain size with greater dose rates and expected palaeodoses due to increased alpha radiation
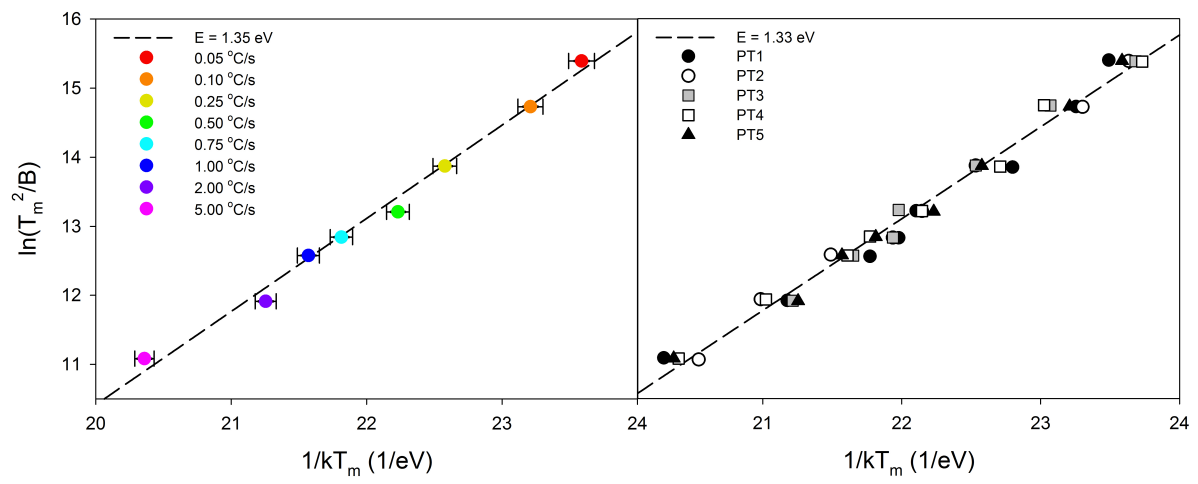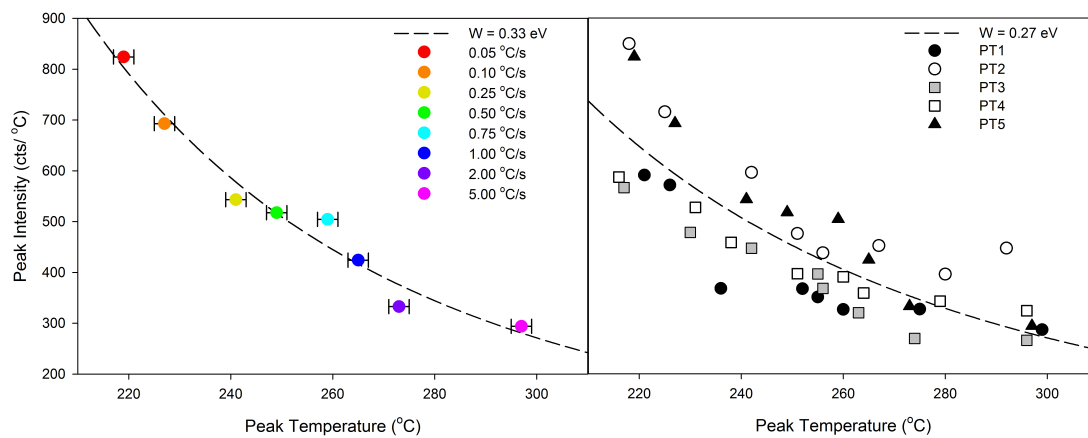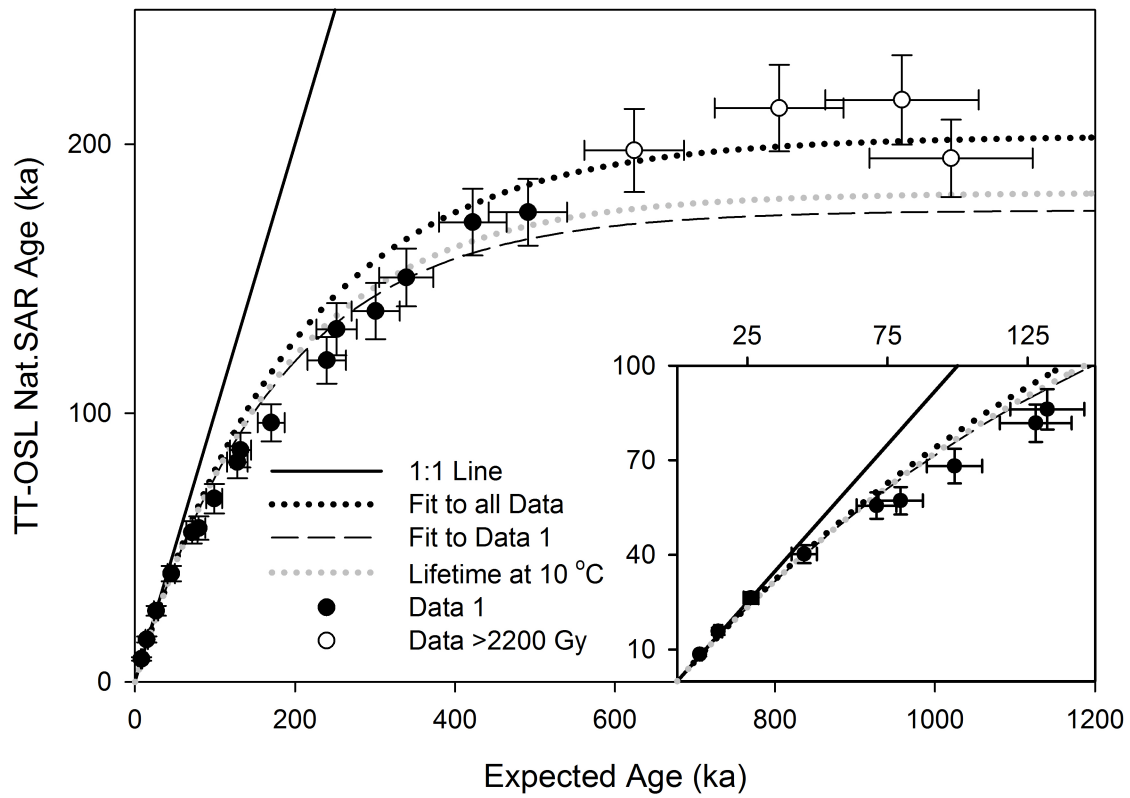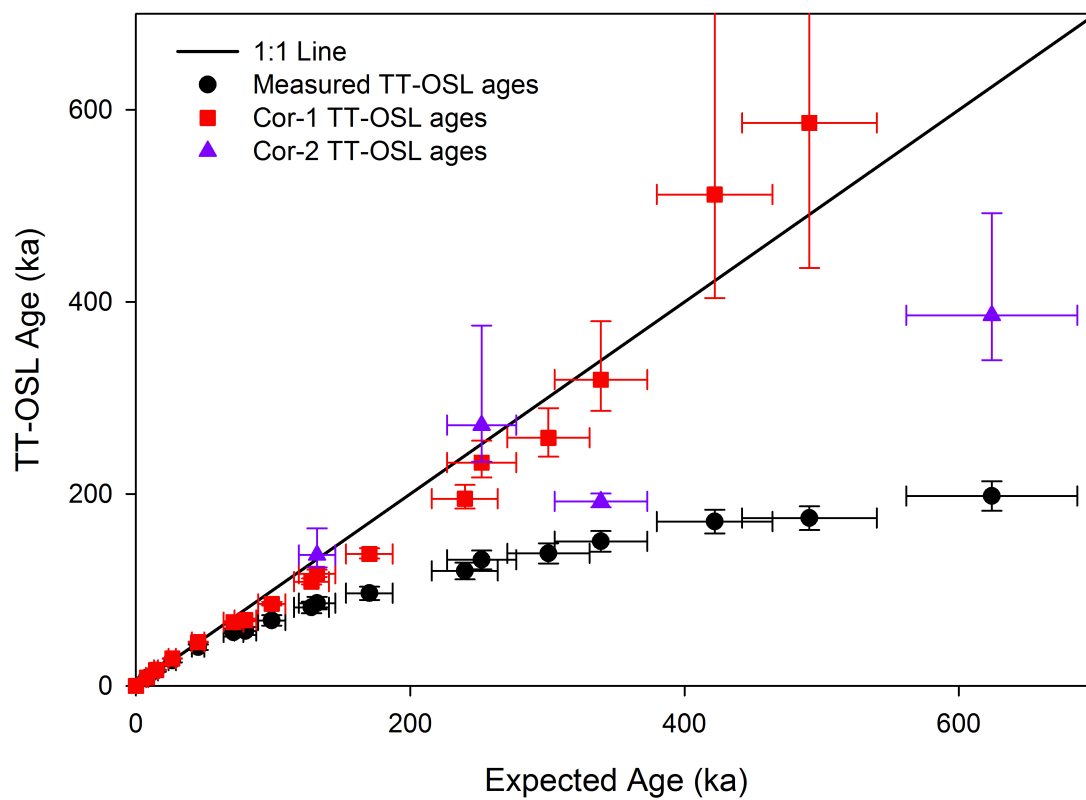
a) TLa
260 °C 10 s
300 s 125 °C OSL

b) TLb
260 °C 10 s
300 s 125 °C OSL
260 °C 10 s
100 s 125 °C OSL

c) TLc
260 °C 10 s
400 s 125 °C OSL

d) TT-OSL
TLa-TLb
TLc-TLb

TL (cts/ °C)

Temperature (°C)
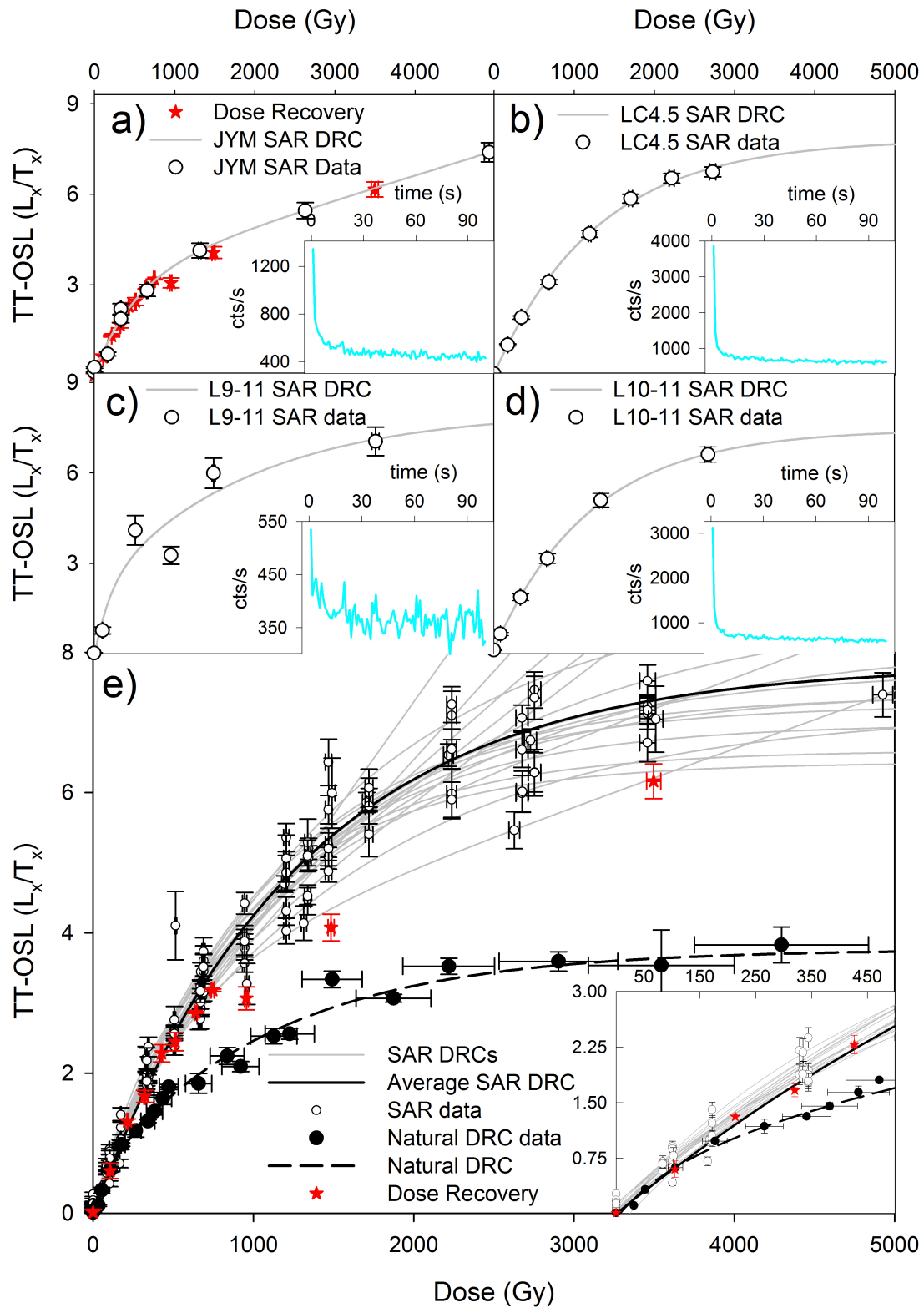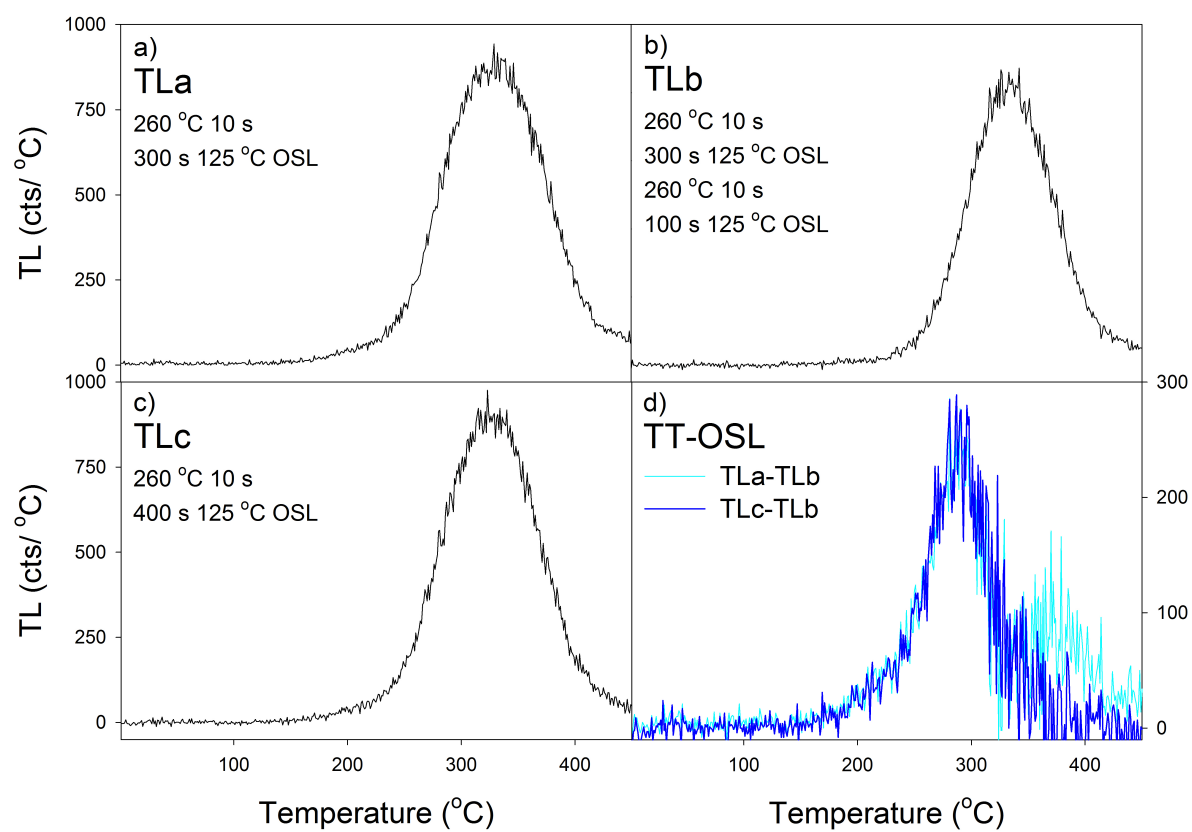
Highlights

- Natural and laboratory TT-OSL DRCs deviate at ~150 Gy but saturate at higher doses
- TT-OSL signal lifetime at 10 °C calculated from measured E and s values is ~180 ka
- TT-OSL signal lifetime at Luochuan estimated from the DRCs' deviation is ~175 ka
- Natural and laboratory TT-OSL DRC deviation may be caused by low thermal stability
- Laboratory measurements of signal lifetime may be able to correct old TT-OSL ages